Joint Channel Estimation and Localization for Cooperative Millimeter Wave Systems

Xi Yang[1], Chao-Kai Wen[2], Shi Jin[1], A. Lee Swindlehurst[3], and Jing Zhang[1]
[1]National Mobile Communications Research Laboratory, Southeast University, Nanjing, P. R. China
[2]Institute of Communications Engineering, National Sun Yat-sen University, Kaohsiung, R.O.C.
[3]Department of Electrical Engineering and Computer Science, University of California, Irvine, Irvine, USA
E-mail: [1]{yangxi, jinshi, jingzhang}@seu.edu.cn, [2]chaokai.wen@mail.nsysu.edu.tw, [3]swindle@uci.edu

***Abstract*—Localization is one of the most interesting topics related to the promising millimeter wave (mmWave) technology. In this paper, we investigate joint channel estimation and localization for a cooperative mmWave system with several receivers. Due to the strong line-of-sight path common to mmWave channels, one can localize the position of the user by exploiting the signal's angle-of-arrival (AoA). Leveraging a variational Bayesian approach, we obtain soft information about the AoA for each receiver. We then use the soft AoA information and geometrical constraints to localize the position of the user and further improve the channel estimation performance. Numerical results show that the proposed algorithm has centimeter-level localization accuracy for an outdoor scene. In addition, the proposed algorithm provides 1-3 dB of gain for channel estimation by exploiting the correlation among the receiver channels depending on the availability of prior information about the path loss model.**

***Index Terms*—Channel estimation, localization, mmWave system, variational Bayesian inference.**

I. Introduction

Millimeter wave (mmWave) communication is a promising technology for future wireless communication systems [1]. Among various topics related to mmWave communication, localization has attracted considerable interest in recent years [2], [3]. The location information of the user enables location-based services such as navigation, mapping, augmented reality, intelligent transportation systems, and so on [4]. Localization techniques can be classified into two main categories: direct and indirect localization [5]. Direct localization uses the received waveform to estimate the location of the user directly [6]. By contrast, indirect localization exploits the channel parameters, such as angle-of-arrival (AoA), to estimate the position of the user. Due to the severe attenuation at high frequencies, wireless channels over the mmWave band often consist of only one or two paths. Hence, channel estimation approaches that exploit channel models based on AoA have better performance than those based for example on least squares [7]–[9].

This work was supported in part by the National Key Research and Development Program 2018YFA0701602 and the National Science Foundation of China under Grant 61941104. The work of C.-K. Wen was supported in part by the Ministry of Science and Technology of Taiwan under grants MOST 108-2628-E-110-001-MY3 and the ITRI in Hsinchu, Taiwan. The work of A. Lee Swindlehurst was supported in part by the U.S. National Science Foundation under Grants CCF-1703635 and ECCS-1824565.

Weighted least squares-based algebraic solutions for the position and velocity of a moving user using time and frequency differences of arrival are investigated in [10]. Reference [11] studied AoA localization with a sensor network, and proposed a closed-form solution using AoAs that can handle the presence of sensor position errors. In [12], the authors investigated localization with distributed antenna arrays and proposed a closed-form positioning method based on the weighted least squares method. Reference [13] investigated downlink positioning with a single reference station that requires both AoA and angle-of-departure measurements which are obtained from the beam training. In [14], the authors studied the localization of users with variable velocities in mmWave systems based on weighted least squares using hybrid AoA, time difference of arrival, and frequency difference of arrival measurements. However, the abovementioned works only consider the localization problem and assume that the channel parameters such as AoA are known at receiver side. Joint channel estimation and localization for mmWave systems has not to date been studied extensively.

In this paper, we focus on joint channel estimation and localization for a cooperative mmWave system with several receivers. The proposed joint channel estimation and localization algorithm consists of three steps. First, the AoA mean direction and concentration parameters are extracted from the received signal for each receiver using a variational Bayesian approach. Secondly, we derive the minimum mean square error (MMSE) and the maximum a posteriori (MAP) estimators to localize the position of the user and refine the AoAs. Finally, the equivalent channel is reconstructed with or without any available prior information about the path loss model. Numerical results show that the proposed joint channel estimation and localization algorithm has centimeter-level localization accuracy for an outdoor scene. By exploiting the correlation among the receiver channels, the proposed algorithm can provide 3 dB of gain in channel estimation with prior information about the path loss model, and 1 dB of gain without.

II. System Model

We consider a mmWave system where a single antenna user is served by L receivers, as shown in Fig. 1. The L receivers are distributed along the x-axis, and each receiver has

978-1-7281-5478-7/20/$31.00

a uniform linear array (ULA) with M antennas. The position of each receiver is known. We further assume line-of-sight (LoS) transmission between the user and L receivers. Fig. 1 shows an instance with five receivers, and the lines between the user and receivers represent the LoS paths. For the i-th receiver, the received signal can be written as

$$\mathbf{y}_i = \mathbf{h}_i s + \mathbf{u}_i = \alpha_i \mathbf{a}(\theta_i) s + \mathbf{u}_i = \beta_i e^{j\psi_i} \mathbf{a}(\theta_i) s + \mathbf{u}_i, \quad (1)$$

where $\mathbf{h}_i$ is the channel between the user and the i-th receiver, α_i is the complex channel coefficient, β_i is the path loss factor, ψ_i is the phase rotation, s is the transmit symbol with $|s|^2 = P_u$, and $\mathbf{u}_i$ is complex Gaussian noise with variance v_u. Assuming that the antenna spacing of each ULA is half wavelength, the steering vector $\mathbf{a}(\theta_i)$ is given by

$$\mathbf{a}(\theta_i) = \left[1, e^{j\pi\cos(\theta_i)}, \cdots, e^{j\pi(M-1)\cos(\theta_i)}\right]^T, \quad (2)$$

where θ_i is the AoA. In this paper, we use the free space path loss model, and thus the path loss factor of the i-th receiver is given as

$$\beta_i = \sqrt{\frac{G_t G_r \lambda^2}{16\pi^2 l_i^2}}, \quad (3)$$

where λ is the wavelength, l_i represents the distance between the user and the i-th receiver, and G_t and G_r denote the antenna gains of the user and receiver, respectively.

For channel estimation, the least squares estimate of $\mathbf{h}_i$ is given by $\hat{\mathbf{h}}_i = \mathbf{y}_i / s$. However, since the channel has a limited number of paths, one can do better by exploiting the channel structure [9]. Specifically, we can obtain a better channel estimate if the AoA and the complex channel gain are directly extracted from the received signal. In addition, we observe that the channels for different ULA receivers are correlated. Correlation is present in the AoAs (θ_i) and the complex channel coefficients (α_i). From Fig. 1 we see that the channels are fully characterized by the position of the user. Given the position of the user (e.g., x- and y-axis coordinates), we can infer the AoA of each ULA. Furthermore, we can use any two AoAs to infer other AoAs, since two AoAs are able to localize the position of the user. Finally, if the position of the user is known, we can use any complex channel coefficient to infer other complex channel coefficients on the basis of the path loss model and the positions of the user and receivers.

In this paper, we focus on joint channel estimation and localization for the considered cooperative mmWave system. We aim to extract the AoAs and the complex channel coefficients, and use the geometrical constraints to estimate the position of the user and improve the channel estimation performance.

III. Joint Channel Estimation and Localization

In this section, we propose a joint channel estimation and localization algorithm. The proposed algorithm has three steps: *a) Extracting the AoAs and the complex channel coefficients*, *b) Localizing the position of the user*, *c) Reconstructing the equivalent channel*. In the following analysis, we detail each step of the proposed algorithm.

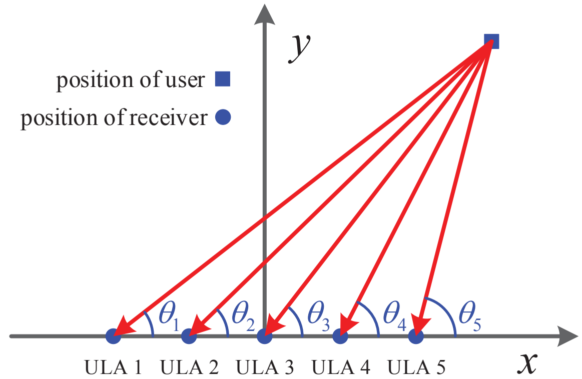

Fig. 1. Model of the considered cooperative mmWave system.

A. Extracting the AoAs and the Complex Channel Coefficients

Equation (1) is a special case of the the fundamental line spectral estimation (LSE) problem. The LSE problem has the following form

$$\mathbf{y} = \mathbf{h} + \mathbf{u} = \sum_{i=1}^{K} \alpha_i \mathbf{s}(\phi_i) + \mathbf{u}, \quad (4)$$

where α_i is the complex amplitude, $\mathbf{u}$ is a complex Gaussian noise vector with independent elements of variance v, and the sinusoid $\mathbf{s}(\phi_i) \in \mathbb{C}^M$ with $\phi_i \in [-\pi, \pi)$ is defined as

$$\mathbf{s}(\phi_i) = \left[1, e^{j\phi_i}, \cdots, e^{j(M-1)\phi_i}\right]^T. \quad (5)$$

Equation (4) consists of several sinusoids, where the complex amplitudes (α_i), the frequencies (ϕ_i), and the model order (K) are unknown. LSE aims to detect the model order K and recover the complex amplitude and the frequency of each sinusoid from the observation $\mathbf{y}$.

For step a), we use the VALSE algorithm [7] to extract the AoA and the complex channel gain of each receiver. The VALSE algorithm solves the fundamental LSE problem on the basis of the probabilistic model and variational Bayesian inference. It assumes that the frequency of each sinusoid follows the von Mises distribution [15]

$$p(\phi_i) = f_{\mathrm{VM}}(\phi_i; \mu, \kappa) = \frac{1}{2\pi I_0(\kappa)} e^{\kappa\cos(\phi_i - \mu)}, \phi_i \in [-\pi, \pi), \quad (6)$$

where μ and κ are the mean direction and the concentration parameters, and $I_p(\cdot)$ is the modified Bessel function of the first kind and order p. The von Mises distribution is of significant importance among distributions on the unit circle, and its role is similar to that of the Gaussian distribution on the line [15]. When $\kappa = 0$, the von Mises distribution degenerates into the uniform distribution on the unit circle. The VALSE algorithm assumes that the complex amplitude follows the Bernoulli-Gaussian distribution

$$p(\alpha_i | \rho, \tau) = (1-\rho)\delta(\alpha_i) + \rho f_{\mathrm{CN}}(\alpha_i; 0, \tau), \quad (7)$$

where ρ is the active rate, $\delta(\cdot)$ is the Dirac delta function, and $f_{\mathrm{CN}}(\alpha_i; 0, \tau)$ is the complex Gaussian distribution

$$f_{\mathrm{CN}}(\alpha_i; 0, \tau) = \frac{1}{\pi\tau} \exp\left(-\frac{|\alpha_i|^2}{\tau}\right), \quad (8)$$

Algorithm 1 VALSE algorithm for LSE problem (14).

Input: Observation $\mathbf{y}$, noise variance v.

Initialization:

1) Initialize the model parameter τ:

$$\hat{\tau} = \frac{1}{M}\mathbf{y}^H\mathbf{y} - v.$$

2) Initialize the frequency ϕ:

$$\mathbf{R} = \frac{2}{Mv}\mathbf{y}\mathbf{y}^H \text{ and } \mathbf{z}_i = \sum_{k=1}^{M} \mathbf{R}_{k,k-i+1}, i = 1, \cdots, M.$$

Use $\mathbf{z}$ as the input of the Heuristic 2 algorithm to obtain $\hat{\mu}$ and $\hat{\kappa}$, and compute

$$\hat{\mathbf{a}} = \left[1, \frac{I_1(\hat{\kappa})}{I_0(\hat{\kappa})}e^{j\hat{\mu}}, \cdots, \frac{I_{M-1}(\hat{\kappa})}{I_0(\hat{\kappa})}e^{j(M-1)\hat{\mu}}\right]^T.$$

while $t < T_{\max}$ **do**

1) Infer the complex amplitude α:

$$\hat{c} = v\left(M + \frac{v}{\hat{\tau}}\right)^{-1} \text{ and } \hat{w} = \frac{\hat{c}}{v}\hat{\mathbf{a}}^H\mathbf{y}.$$

2) Estimate the model parameter τ:

$$\hat{\tau} = |\hat{w}|^2 + \hat{c}.$$

3) Infer the frequency ϕ:
Use $\mathbf{z} = \frac{2\hat{w}^*}{v}\mathbf{y}$ as the input of the Heuristic 2 algorithm to obtain $\hat{\mu}$ and $\hat{\kappa}$, and compute

$$\hat{\mathbf{a}} = \left[1, \frac{I_1(\hat{\kappa})}{I_0(\hat{\kappa})}e^{j\hat{\mu}}, \cdots, \frac{I_{M-1}(\hat{\kappa})}{I_0(\hat{\kappa})}e^{j(M-1)\hat{\mu}}\right]^T.$$

Output: $\hat{\mu}$, $\hat{\kappa}$, $\hat{w}$, and $\hat{\mathbf{a}}$.

where τ is the amplitude.

In the LSE problem, there are at most N ($N \leq M$) possible sinusoids, and only K ($K < N$) sinusoids are active. Equation (7) is a sparsity-promoting prior. Hence, we have

$$\mathbf{y} = \mathbf{h} + \mathbf{u} = \sum_{i=1}^{N} \alpha_i \mathbf{s}(\phi_i) + \mathbf{u}, \tag{9}$$

and we have the following joint pdf

$$p(\mathbf{y}, \phi_1, \cdots, \phi_N, \alpha_1, \cdots, \alpha_N, \rho, \tau, v) = f_{\mathrm{CN}}\left(\mathbf{y}; \sum_{i=1}^{N} \alpha_i \mathbf{s}(\phi_i), v\mathbf{I}\right) \prod_{i=1}^{N} p(\phi_i) p(\alpha_i | \rho, \tau). \tag{10}$$

According to the mean field approximation, we have the following surrogate pdf

$$q(\phi_1,\cdots,\phi_N,\alpha_1,\cdots,\alpha_N|\mathbf{y}) = q(\alpha_1, \cdots, \alpha_N|\mathbf{y}) \prod_{i=1}^{N} q(\phi_i|\mathbf{y}), \tag{11}$$

where $q(\phi_i|\mathbf{y})$ and $q(\alpha_1, \cdots, \alpha_N|\mathbf{y})$ are restricted to the families of candidate pdfs:

$$q(\phi_i|\mathbf{y}) = f_{\mathrm{VM}}(\phi_i; \hat{\mu}_i, \hat{\kappa}_i), \tag{12}$$

$$q(\alpha_1, \cdots, \alpha_N|\mathbf{y}) = f_{\mathrm{CN}}\left(\alpha_1, \cdots, \alpha_N; \hat{\mathbf{w}}, \hat{\mathbf{C}}\right). \tag{13}$$

Using variational Bayesian inference, the VALSE algorithm iteratively reduces the KL divergence between the joint pdf (10) and the surrogate pdf (11) by updating the parameters of (12) and (13). The model parameters ρ, τ, and v are also estimated iteratively in the VALSE algorithm.

Since the considered model (1) only has one sinusoid, we can formulate the LSE problem

$$\mathbf{y} = \mathbf{h} + \mathbf{u} = \alpha\mathbf{s}(\phi) + \mathbf{u} \tag{14}$$

with the surrogate pdf

$$q(\phi, \alpha|\mathbf{y}) = q(\alpha|\mathbf{y})q(\phi|\mathbf{y}) = f_{\mathrm{VM}}(\phi; \hat{\mu}, \hat{\kappa}) f_{\mathrm{CN}}(\alpha; \hat{w}, \hat{c}), \tag{15}$$

where the noise variance v is known. In addition, ϕ follows the uniform distribution in $[-\pi, \pi)$. Algorithm 1 details the channel estimation procedure, which can be derived from the original VALSE algorithm. In Algorithm 1, we have $\hat{\mathbf{a}} = \mathrm{E}\{\mathbf{s}(\phi)\}$, where the expectation is taken over the von Mises distribution $f_{\mathrm{VM}}(\phi; \hat{\mu}, \hat{\kappa})$. In addition, the channel estimate is given as $\hat{\mathbf{h}} = \hat{w}\hat{\mathbf{a}}$. Note that we use the Heuristic 2 algorithm of [7] to update the parameters $\hat{\mu}$ and $\hat{\kappa}$. Please see Section IV-D of [7] for details. Note that the prior distributions (6) and (7) are defined for computation convenience. In practice, it does not require the channel actually follows such prior distribution model [7].

B. Localizing the Position of the User

The VALSE algorithm extracts the complex amplitude and the frequency from the received signal by exploiting the channel structure. According to (2) and (5), the estimate of the AoA of the i-th receiver can be obtained as

$$\hat{\theta}_i = \arccos\left(\frac{\hat{\mu}_i}{\pi}\right), \tag{16}$$

where $\hat{\mu}_i$ is the estimate of the frequency from Algorithm 1 given the received signal $\mathbf{y}_i$. However, Algorithm 1 not only provides the mean direction $\hat{\mu}_i$ but also the concentration parameter $\hat{\kappa}_i$, which describes the accuracy of the frequency estimate $\hat{\mu}_i$. Fig. 2 illustrates the von Mises distributions with $\mu = 0$ and different concentration parameters κ. We see that a larger concentration parameter implies a better estimate of the mean direction. The soft information provided by Algorithm 1 can help to localize the user. Using this information, we can characterize the spatial distribution of the user along with the geometrical constraints.

At first, we provide the deterministic geometrical constraints among the AoAs of the receivers. As shown in Fig. 1, we use ULA 1 to denote the left-most array at point $(-d, 0)$ and ULA L to denote the right-most array at point $(d, 0)$. Other ULAs are distributed between ULA 1 and ULA L. We use θ_1 and θ_L to denote the AoAs of ULA 1 and ULA L, respectively. Using the geometrical constraints, the AoA θ_i of the i-th ULA at point $(d_i, 0)$ can be derived as

$$\theta_i = f_\theta(\theta_1, \theta_L, d_i) = \arccos\left(\frac{\frac{d-d_i}{2d}\cot(\theta_1) + \frac{d+d_i}{2d}\cot(\theta_L)}{\sqrt{1 + \left(\frac{d-d_i}{2d}\cot(\theta_1) + \frac{d+d_i}{2d}\cot(\theta_L)\right)^2}}\right), \tag{17}$$

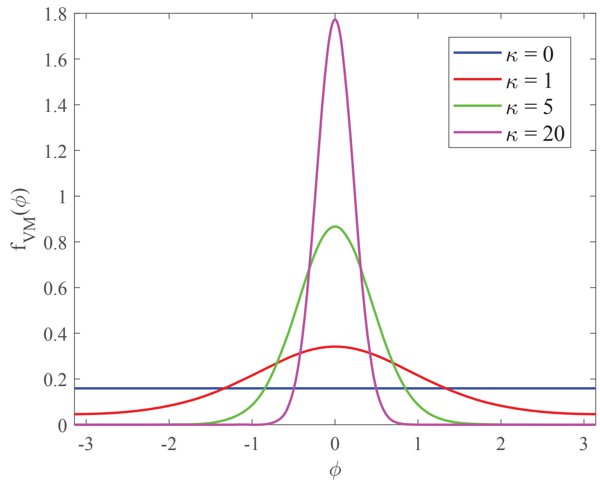

Fig. 2. The von Mises distributions with mean direction $\mu = 0$ and different concentration parameters κ.

where $-d \leq d_i \leq d$. Equation (17) shows that we can use two AoAs to infer other AoAs when the positions of the receivers are fixed. The corresponding sinusoidal frequency is given as

$$\phi_i = f_\phi(\theta_1, \theta_L, d_i) = \pi\cos(\theta_i), \tag{18}$$

where θ_i is defined as (17). Hence, the spatial distribution of the user can be characterized by the joint pdf

$$p_{\rm u}(\theta_1, \theta_L) = \frac{1}{C}\prod_{i=1}^{L} f_{\rm VM}(f_\phi(\theta_1, \theta_L, d_i); \hat{\mu}_i, \hat{\kappa}_i), \tag{19}$$

where $0 < \theta_1 < \theta_L < \pi$, $\hat{\mu}_i$ and $\hat{\kappa}_i$ are the estimated parameters of i-th receiver obtained from Algorithm 1, and C is a normalizing constant. Based on the joint pdf (19), we can localize the position of the user and refine the estimate of the AoAs and steering vectors.

1) MMSE estimate: The MMSE estimate of the AoA is given by

$$\hat{\theta}_i^{\rm mmse} = \int_0^\pi \int_{\theta_1}^\pi f_\theta(\theta_1, \theta_L, d_i) p_{\rm u}(\theta_1, \theta_L) d\theta_1 d\theta_L. \tag{20}$$

Given θ_1 and θ_L, the position of the user can be derived as

$$x_{\rm u} = f_{\rm x}(\theta_1, \theta_L) = \frac{\tan(\theta_1) + \tan(\theta_L)}{\tan(\theta_L) - \tan(\theta_1)} d, \tag{21}$$

$$y_{\rm u} = f_{\rm y}(\theta_1, \theta_L) = \frac{2\tan(\theta_1)\tan(\theta_L)}{\tan(\theta_L) - \tan(\theta_1)} d. \tag{22}$$

Therefore, the MMSE estimate of the user position is given by

$$\hat{x}_{\rm u}^{\rm mmse} = \int_0^\pi \int_{\theta_1}^\pi f_{\rm x}(\theta_1, \theta_L) p_{\rm u}(\theta_1, \theta_L) d\theta_1 d\theta_L, \tag{23}$$

$$\hat{y}_{\rm u}^{\rm mmse} = \int_0^\pi \int_{\theta_1}^\pi f_{\rm y}(\theta_1, \theta_L) p_{\rm u}(\theta_1, \theta_L) d\theta_1 d\theta_L. \tag{24}$$

Note that (20), (23), and (24) must generally be calculated by numerical integration.

2) MAP estimate: The MAP estimate of the AoA is given by

$$\left(\hat{\theta}_1^{\rm map}, \hat{\theta}_L^{\rm map}\right) = \arg\max_{\theta_1, \theta_L}\{p_{\rm u}(\theta_1, \theta_L)\}. \tag{25}$$

Given $\hat{\theta}_1^{\rm map}$ and $\hat{\theta}_L^{\rm map}$, we can use (17) to obtain the MAP estimates of other AoAs, and use (21) and (22) to obtain the MAP estimate of the position $(\hat{x}_{\rm u}^{\rm map}, \hat{y}_{\rm u}^{\rm map})$ of the user. The MAP estimates can be obtained by searching the grid points in the region of $0 < \theta_1 < \theta_L < \pi$.

C. Reconstructing the Equivalent Channel

Step a) and step b) jointly localize the position of the user and refine the estimates of the AoAs. In step c), we provide two approaches to reconstruct the equivalent channel. First, we reconstruct the steering vector $\mathbf{a}(\hat{\theta}_i)$ according to $\hat{\theta}_i^{\rm mmse}$ or $\hat{\theta}_i^{\rm map}$, and then focus on the complex channel coefficient. If the path loss model is unknown, we can use the least squares estimate to obtain

$$\hat{\alpha}_i = \frac{1}{M}\mathbf{a}^H(\hat{\theta}_i)\mathbf{y}_i. \tag{26}$$

If the path loss model is known, we can use the position of the user to go further. The estimate of the path loss factor under the free space path loss model is given as

$$\hat{\beta}_i = \sqrt{\frac{G_t G_r \lambda^2}{16\pi^2\left(\left(\hat{x}_u - d_i\right)^2 + \hat{y}_{\rm u}^2\right)}}. \tag{27}$$

The phase rotation can be obtained using the least squares estimate

$$\hat{\psi}_i = \arg\left(\mathbf{a}^H(\hat{\theta}_i)\mathbf{y}_i\right), \tag{28}$$

and we have $\hat{\alpha}_i = \hat{\beta}_i e^{j\hat{\psi}_i}$. Finally, the equivalent channel is given as $\hat{\mathbf{h}}_i = \hat{\alpha}_i \mathbf{a}(\hat{\theta}_i)$.

IV. Numerical results

In this section, the proposed joint channel estimation and localization algorithm is verified through computer simulations. There are five receivers, where each receiver has 8 antennas and the positions of the receivers are $d_1 = -16$ m, $d_2 = -8$ m, $d_3 = 0$ m, $d_4 = 8$ m, and $d_5 = 16$ m. The position of the user is uniformly randomly generated in a rectangular region defined by -20 m $\leq x_{\rm u} \leq 20$ m and 5 m $\leq y_{\rm u} \leq 40$ m. The system operates at 28 GHz with a 100 MHz bandwidth, the power spectral density of the AWGN is -174 dBm/Hz, and we have $G_t = G_r = 1$. Since the MMSE and MAP estimates have nearly the same performance, we only show the performance of the MAP estimate.

Fig. 3 shows the channel estimation performance of all receivers for the different algorithms. For case I, we only perform Algorithm 1, i.e. step a), for each receiver. For case II and case III, we perform the proposed joint channel estimation and localization algorithm, which includes step a), b), and c), with and without knowledge of path loss model. Case IV also shows the performance of the proposed algorithm, but we use the exact complex channel coefficient α to obtain

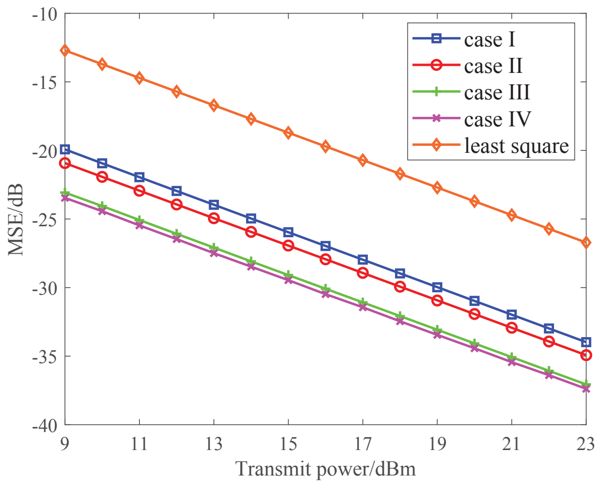

Fig. 3. Channel estimation performance of different algorithms.

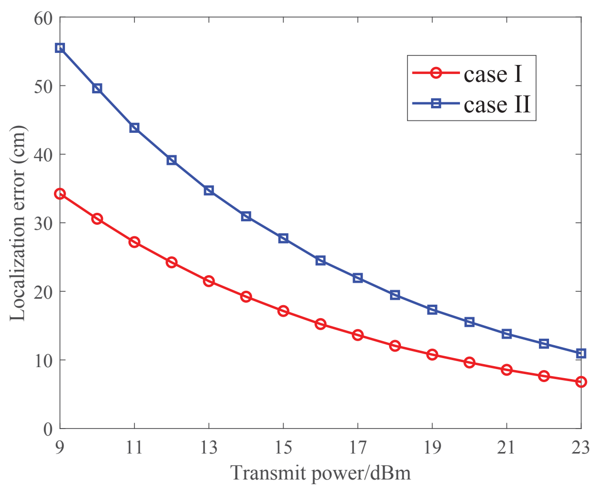

Fig. 4. Localization performance of different cases.

the equivalent channel in step c). We find that the proposed algorithm can improve the channel estimation performance by exploiting the correlation among the channels. Case II provides approximately 1 dB gain. With knowledge of the path loss model, case III provides nearly 3 dB gain. Compared with case III, reconstructing the equivalent channel with the exact α only slightly improves the channel estimation performance. In addition, estimating the channel with channel structure information significantly outperforms the least squares estimate.

Fig. 4 shows the average localization error for two cases. Case I is the proposed joint channel estimation and localization algorithm. As a comparison, case II shows the localization performance with a single receiver positioned at $(0, 0)$. This receiver has a ULA with $8 \times 5 = 40$ antennas. We assume that the path loss model is known. We use Algorithm 1 to extract the AoA $\hat{\theta}_i$ and the complex channel coefficient $\hat{\alpha}_i$, and use the path loss model to estimate the distance between the user and the receiver

$$\hat{l}_i = \sqrt{\frac{G_t G_r \lambda^2}{16\pi^2 |\hat{\alpha}_i|^2}}. \tag{29}$$

Although case II has a single ULA with much higher resolution, we find that case I can provide better localization performance by exploiting the correlation. In addition, if the path loss model is unknown, we cannot localize the position of the user with a single ULA if we only utilize the information from channel estimation.

V. Conclusion

In this study, we proposed a joint channel estimation and localization algorithm for a cooperative mmWave system with several receivers. We derived the MMSE and MAP estimators to obtain the position of the user and refine the estimates of the AoAs on the basis of the geometrical constraints and the soft AoA information extracted from the received signals. Given the estimates of the AoAs, the equivalent channel was reconstructed with and without prior information about the path loss model. Numerical results showed that the proposed algorithm not only provides centimeter-level localization accuracy, but also improves the channel estimation performance.

References

[1] F. Boccardi, R. W. Heath, A. Lozano, T. L. Marzetta, and P. Popovski, "Five disruptive technology directions for 5G," *IEEE Commun. Mag.*, vol. 52, no. 2, pp. 74-80, Feb. 2014.

[2] F. Lemic, J. Martin, C. Yarp, D. Chan, V. Handziski, R. Brodersen, G. Fettweis, A. Wolisz, and J. Wawrzynek, "Localization as a feature of mmWave communication," in *Proc. IEEE IWCMC*, Sep. 2016, pp. 1033-1038.

[3] H. Wymeersch, G. Seco-Granados, G. Destino, D. Dardari, and F. Tufvesson, "5G mmWave positioning for vehicular networks," *IEEE Wireless Commun.*, vol. 24, no. 6, pp. 80-86, Dec. 2017.

[4] J. A. del Peral-Rosado, R. Raulefs, J. A. López-Salcedo, and G. Seco-Granados, "Survey of cellular mobile radio localization methods: From 1G to 5G," *IEEE Commun. Surv. Tutor.*, vol. 20, no. 2, pp. 1124-1148, May 2018.

[5] F. Wen, H. Wymeersch, B. Peng, W. P. Tay, H. C. So, and D. Yang, "A survey on 5G massive MIMO localization," *Digit. Signal Process*, 2019, https://doi.org/10.1016/j.dsp.2019.05.005.

[6] N. Garcia, H. Wymeersch, E. G. Larsson, A. M. Haimovich, and M. Coulon, "Direct localization for massive MIMO," *IEEE Trans. Signal Process.*, vol. 65, no. 10, pp. 2475-2487, May 2017.

[7] M. Badiu, T. L. Hansen, and B. H. Fleury, "Variational Bayesian inference of line spectra," *IEEE Trans. Signal Process.*, vol. 65, no. 9, pp. 2247-2261, May 2017.

[8] C.-J. Wang, C.-K. Wen, S. Jin, and S.-H. Tsai, "Gridless channel estimation for mixed one-bit antenna array systems," *IEEE Trans. Wireless Commun.*, vol. 17, no. 12, pp. 8485-8501, Dec. 2018.

[9] S. Rao, A. Mezghani, and A. L. Swindlehurst, "Channel estimation in one-bit massive MIMO systems: Angular versus unstructured models," *IEEE J. Sel. Topics Signal Process.*, vol. 13, no. 5, pp. 1017-1031, Sep. 2019.

[10] K. C. Ho and W. W. Xu, "An accurate algebraic solution for moving source location using TDoA and FDoA measurements," *IEEE Trans. Signal Process.*, vol. 52, no. 9, pp. 2453-2463, Aug. 2004.

[11] Y. Wang and K. C. Ho, "An asymptotically efficient estimator in closed-form for 3-D AOA localization using a sensor network," *IEEE Trans. Wireless Commun.*, vol. 14, no. 12, pp. 6524-6535, Jul. 2015.

[12] R. Amiri, F. Behnia, and H. Zamani, "Efficient 3-D positioning using time-delay and AoA measurements in MIMO radar systems," *IEEE Commun. Lett.*, vol. 21, no. 12, pp. 2614-2617, Aug. 2017.

[13] H. Wymeersch, N. Garcia, H. Kim, G. Seco-Granados, S. Kim, F. Wen, and M. Fröhle, "5G mmWave downlink vehicular positioning," in *Proc. IEEE GLOBECOM*, Dec. 2018, pp. 1-6.

[14] J. Yang, S. Jin, C.-K. Wen, J. Guo, and M. Matthaiou, "3-D Positioning and Environment Mapping for mmWave Communication Systems," *arXiv preprint arXiv: 1908.04142*, 2019.

[15] K. V. Mardia and P. E. Jupp, *Directional Statistics*. New York, NY, USA: Wiley, 2000.